To boldly go where no microRNAs have gone before: Spaceflight impact on risk for small-for-gestational-age infants

Giada Corti, JangKeun Kim, Francisco J. Enguita, Joseph W. Guarnieri, Lawrence I. Grossman, Sylvain V. Costes, Matias Fuentealba, Ryan T. Scott, Andrea Magrini, Lauren M. Sanders, David Furman, Jean Calleja-Agius, Christopher E. Mason, Diego Galeano, Massimo Bottini, Afshin Beheshti

Table of Contents

Additional Supplemental Material

Supplementary Data 1. Data from the GSEA pathway analysis on blood samples from C57BL/6 mice 14 days post exposure to 50 cGy simplified GCR simulated irradiation
Supplementary Data 2. Gene targets for all 13 miRNAs.
Supplementary Data 3. Data from the GSEA pathway sex specific analysis on blood samples from Inspiration4 (I4) astronauts with the Hallmark, Reactome, and MitoPathway databases.
Supplementary Data 4. Predicted small molecule drugs for SGA-associated spaceflight miRNA signature.

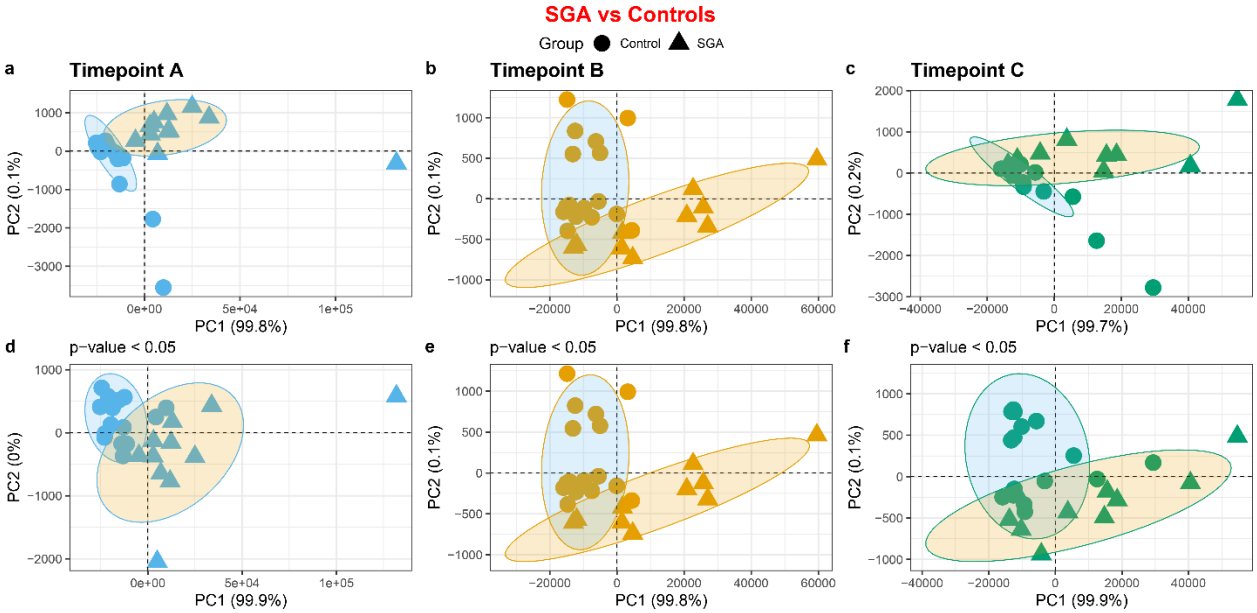

Supplementary Figure 1. Global miRNA expression response in SGA patients vs. controls across gestation timepoints. Principal Component Analysis (PCA) plots illustrating the overall miRNA expression patterns in Small-for-Gestational-Age (SGA) patients (triangles) compared to control (healthy) patients (circles) at three gestation timepoints: A (blue), B (yellow), and C (green). Panels **a)** to **c)** display PCA plots for all miRNAs, while panels **d)** to **f)** focus on miRNAs with statistical significance ($p < 0.05$). The distinct clustering indicates differential miRNA expression profiles between SGA and control groups at each timepoint.

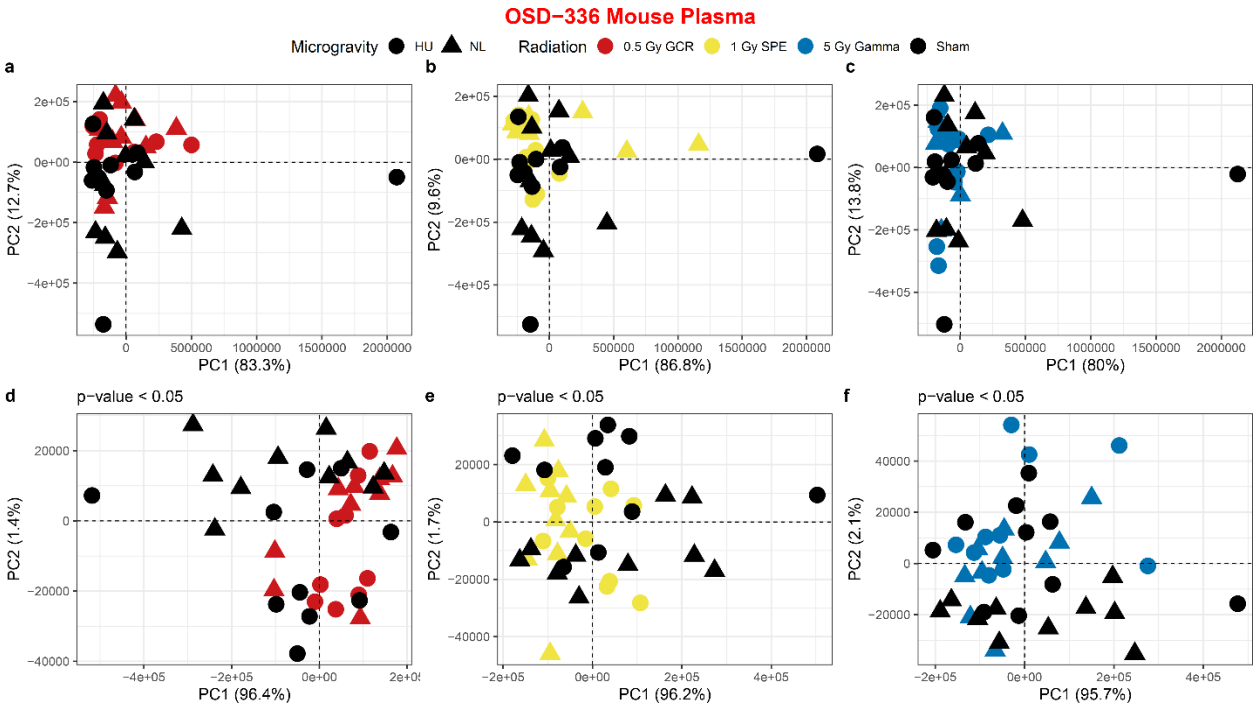

Supplementary Figure 2. Global miRNA expression in irradiated mice vs. sham controls. Principal Component Analysis (PCA) plots depict overall miRNA expression patterns in mice exposed to different radiation doses: 0.5 Gy GCR (red), 1 Gy SPE (yellow), and 5 Gy gamma (blue), compared to 0 Gy sham controls (black). Panels (**a-c**) present PCA plots for all miRNAs, while panels (**d-f**) focus on miRNAs with statistical significance ($p < 0.05$). Distinct clustering signifies differential miRNA expression profiles between irradiated and 0 Gy sham groups

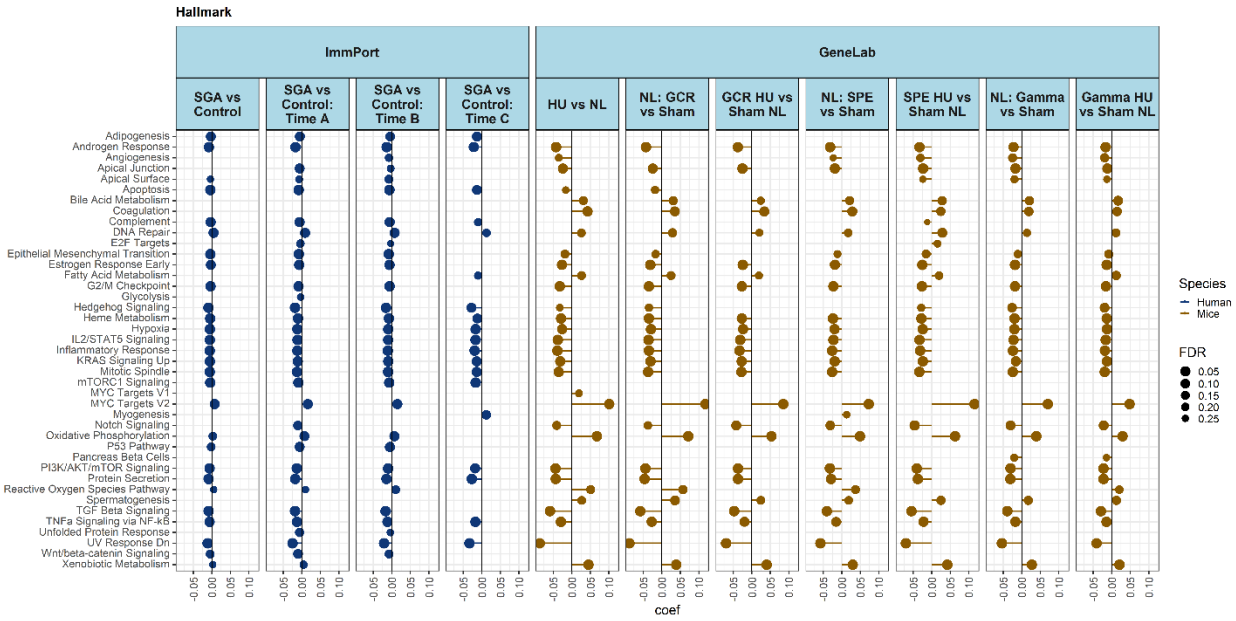

Supplementary Figure 3. Global miRNA pathway analysis on Hallmark pathways. Gene set analysis of miRNAs on Hallmark pathways in Small for Gestational Age (SGA) and simulated spaceflight pathways compared to control. SGA human miRNA regulation is compared to control both time-independently and at different timepoints (left). Space radiation miRNAs with and without simulated microgravity are compared to Sham (right). The x-axis represents a coefficient term indicating pathway inhibition (negative value) or activation (positive value). The point size indicates the degree of significance, denoted by False Discovery Rate (FDR). Only significant values (FDR < 0.25) are displayed.

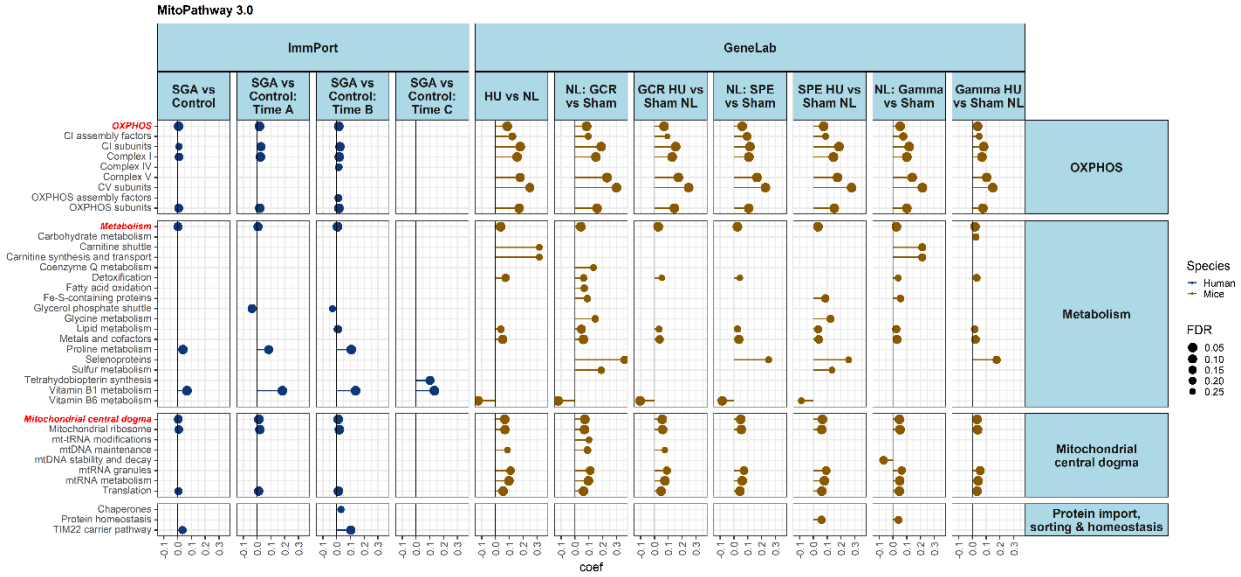

Supplementary Figure 4. Global miRNA pathway analysis on MitoPathways. Gene set analysis of miRNAs on MitoPathways in Small for Gestational Age (SGA) and simulated spaceflight pathways compared to control. SGA human miRNA regulation is compared to control both time-independently and at different timepoints (left). Space radiation miRNAs with and without simulated microgravity are compared to Sham (right). The x-axis represents a coefficient term indicating pathway inhibition (negative value) or activation (positive value). The point size indicates the degree of significance, denoted by False Discovery Rate (FDR). Only significant values (FDR < 0.25) are displayed.

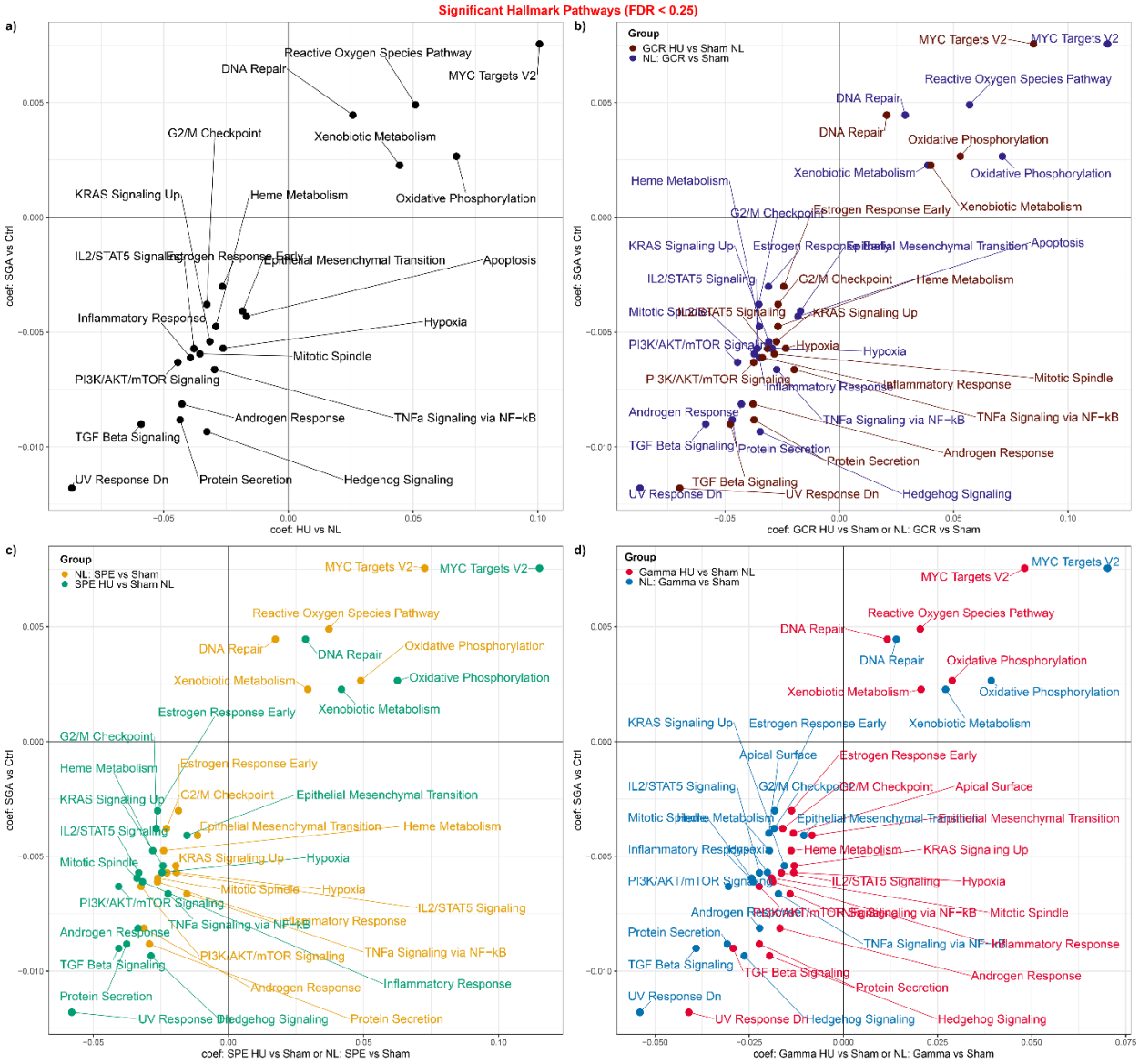

Supplementary Figure 5. Common Global miRNA pathway analysis on Hallmark pathways. Scatter plot of the common significant gene sets (FDR < 0.25) analysis of miRNAs on Hallmark pathways in Small for Gestational Age (SGA) vs. Controls (y-axis) compared to **a)** Hindlimb Unloading (HU) vs. Normal Loaded (NL), **b)** all GCR conditions vs. Sham NL, **c)** all SPE conditions vs. Sham NL, and **d)** all gamma conditions vs Sham NL.

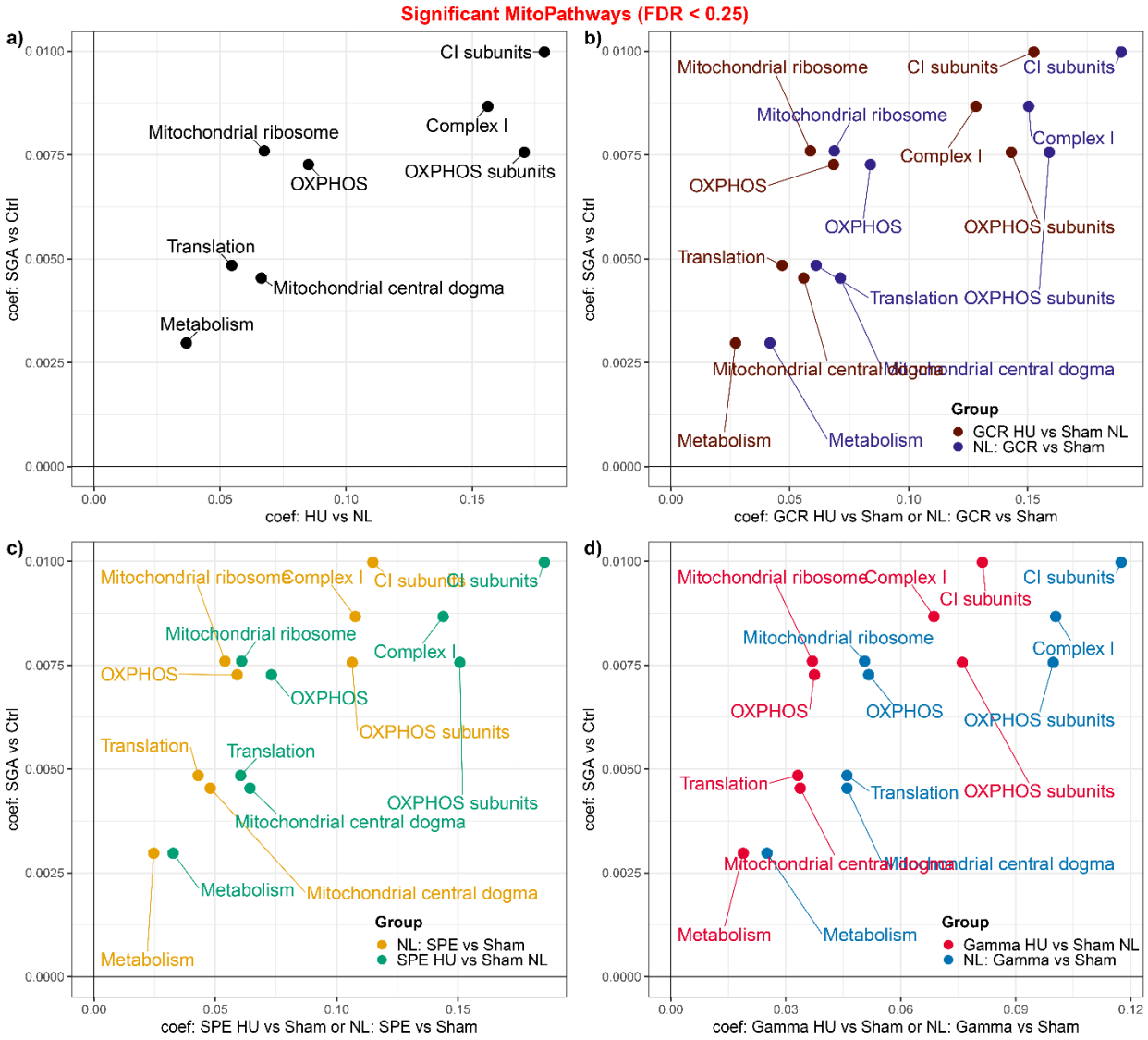

Supplementary Figure 6. Common Global miRNA pathway analysis on MitoPathways. Scatter plot of the common significant gene sets (FDR < 0.25) analysis of miRNAs on MitoPathways in Small for Gestational Age (SGA) vs. Controls (y-axis) compared to **a)** Hindlimb Unloading (HU) vs. Normal Loaded (NL), **b)** all GCR conditions vs. Sham NL, **c)** all SPE conditions vs. Sham NL, and **d)** all gamma conditions vs Sham NL.

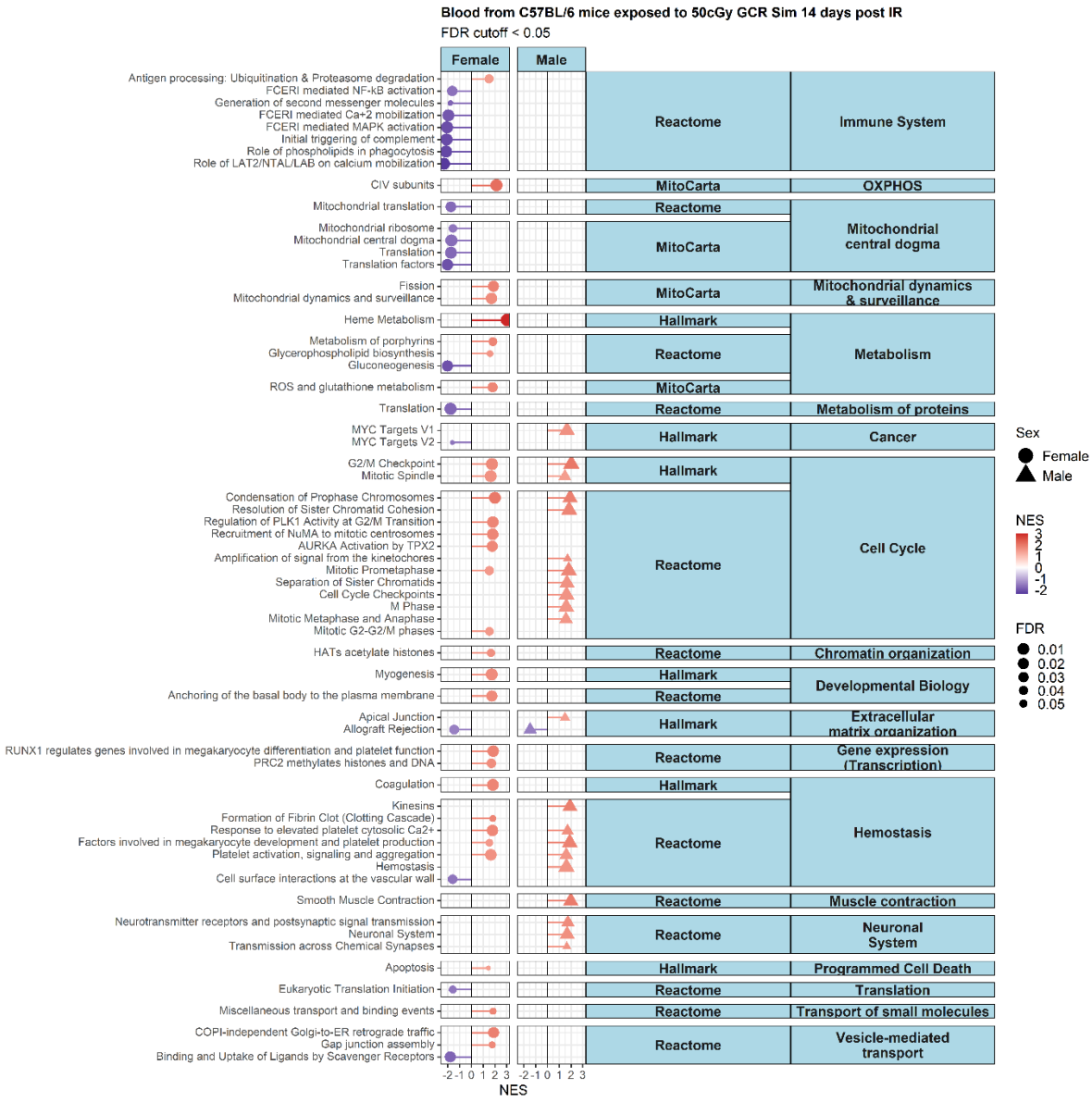

Supplementary Figure 7. Pathways similar to the 13 miRNA gene target pathways from Fig. 4 from analysis on blood samples from C57BL/6 mice 14 days post exposure to 50 cGy simplified GCR simulated irradiation. This lollipop plot represents fast Gene Set Enrichment Analysis (fGSEA) of differential gene expression (DGE) data from blood samples of 24-week-old male and female C57BL/6 mice. The mice were exposed to 50 cGy of simplified GCR simulated irradiation, and blood samples were collected 14 days post-exposure for RNA sequencing. fGSEA was performed using the Hallmark, Reactome, and MitoCarta pathway databases. The plot highlights pathways similar to those identified in the functional pathway analysis of the 13 miRNAs in **Figure 4**, showing that similar pathways are dysregulated in female and male mice 14 days after exposure to simulated space radiation. The x-axis represents the Normalized Enrichment Score (NES), with negative values (shades of blue) indicating pathway inhibition and positive values (shades of red) indicating pathway activation. Point size reflects the degree of significance, denoted by the False Discovery Rate (FDR). Only significant values (FDR < 0.05) are displayed. The complete list of pathway analyses is available in **Supplementary Data 1**.

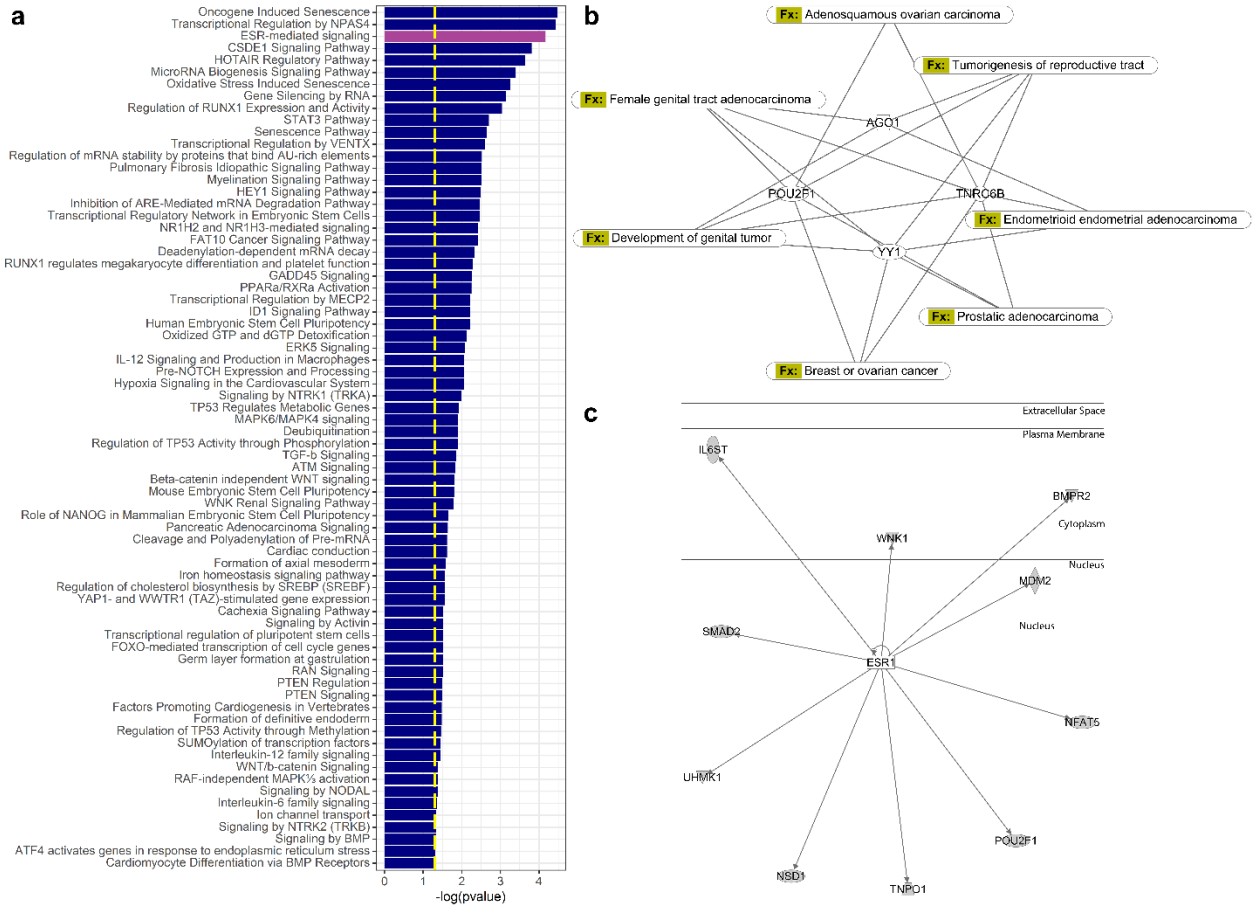

Supplementary Figure 8. Pathway analysis with Ingenuity Pathway Analysis (IPA) on the 45 gene targets shared by 10 or more of the 13 miRNAs. a) Canonical Pathway analysis by IPA software showing the top enriched network based on 45 gene targets shared by 10 or more of the 13 miRNAs in this study. The –log(p-value) (Fisher's Exact Test) is displayed with the dashed yellow representing p-value < 0.05. ESR related pathway is shown in magenta. **b)** The 4 genes *AGO1*, *POU2F1*, *TNRC6B*, and *YY1* identified to be associated with (ESR)-mediated signaling were predicted to be involved in reproductive system diseases. The network was created using the disease and function overlap feature of IPA. **c)** Upstream regulator analysis of 45 gene targets shared by 10 or more of the 13 miRNAs in this study. Results indicated 10 potential genes regulated by ESR1 in different cellular compartments.

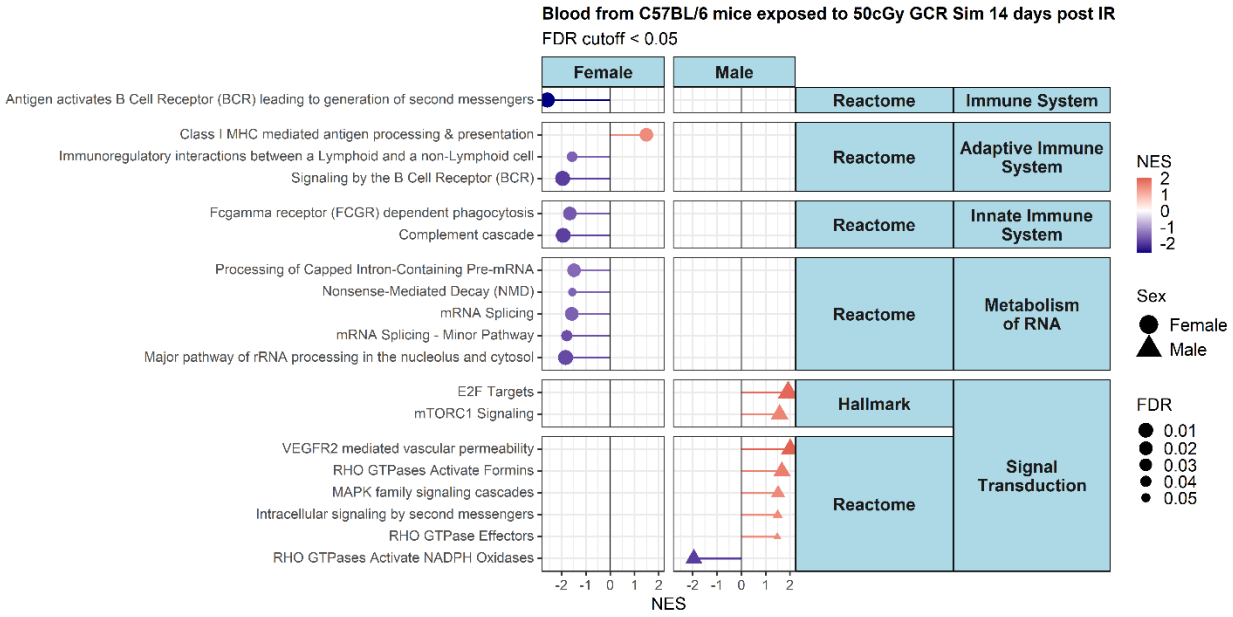

Supplementary Figure 9. Pathways similar to the 45 gene target pathways from Fig. 5 from analysis on blood samples from C57BL/6 mice 14 days post exposure to 50 cGy simplified GCR simulated irradiation. This lollipop plot represents fast Gene Set Enrichment Analysis (fGSEA) of differential gene expression (DGE) data from blood samples of 24-week-old male and female C57BL/6 mice. The mice were exposed to 50 cGy of simplified GCR simulated irradiation, and blood samples were collected 14 days post-exposure for RNA sequencing. fGSEA was performed using the Hallmark and Reactome pathway databases. The plot highlights pathways similar to those identified for the 45 gene targets for the 13 miRNAs in **Figure 5**, showing that similar pathways are dysregulated in female and male mice 14 days after exposure to simulated space radiation. The x-axis represents the Normalized Enrichment Score (NES), with negative values (shades of blue) indicating pathway inhibition and positive values (shades of red) indicating pathway activation. Point size reflects the degree of significance, denoted by the False Discovery Rate (FDR). Only significant values (FDR < 0.05) are displayed. The complete list of pathway analyses is available in **Supplementary Data 1**.

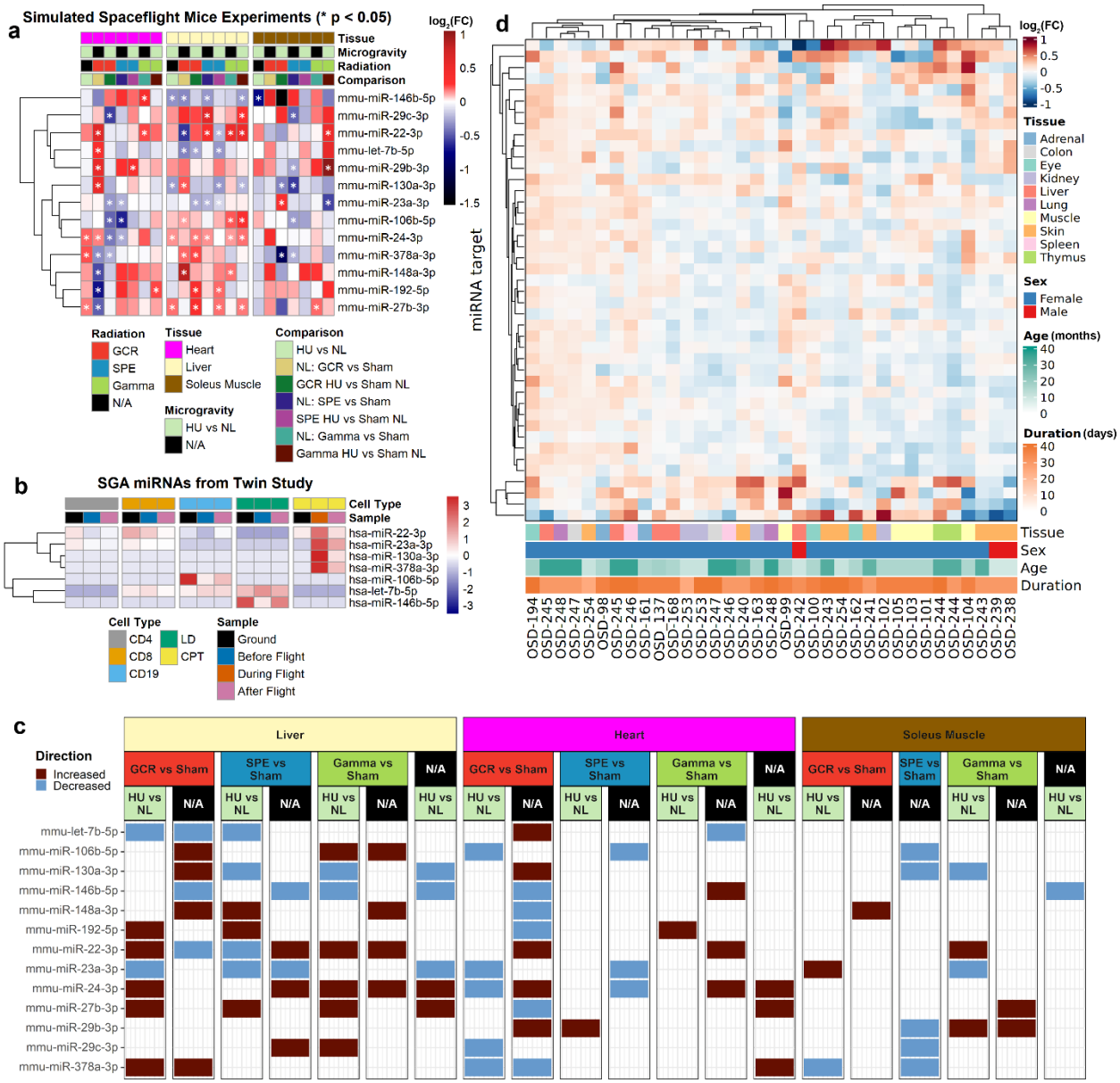

Supplementary Figure 10. The impact of the 13 miRNAs and top 45 gene targets on other tissues exposed to the space environment. a) Heatmap displaying the $\log_2$(fold change) values for the 13 key miRNAs on heart, liver, and soleus muscle from mice exposed to simulated spaceflight experiments 24 hours after irradiation. For the heatmap, $\log_2$(Fold-Change) is color-coded, with red shades indicating upregulated genes and blue shades indicating downregulated genes. Significance is denoted by * p-value < 0.05. **b)** The miRNAs present from the 13 miRNAs in the NASA Twins Study data for CD4 cells, CD8 cells, CD19 cells, lymphocyte depleted cells (LD) and unsorted PBMCs (CPT) comparing before flight, during flight, after flight, and ground controls (i.e. Twin on Earth). The values shown are the miRNA expression values normalized across each miRNA. **c)** Bar plot displaying the 13 miRNAs significantly either increased (brick red) or decreased (blue) in expression in the liver, heart, and soleus muscle from mice exposed to the space environment 24 hours after irradiation. **d)** Top 45 gene targets for the 13 miRNAs across various tissues from mice exposed to the microgravity environment of the International

Space Station (ISS). Analysis was conducted on the top 45 genes using 35 distinct datasets from NASA's Open Science Data Repository (OSDR), encompassing mice flown to the ISS at varying ages, durations in space, and sexes. The heatmap visually represents the $\log_2$(fold-change) values for the genes, with upregulated genes depicted in shades of red and downregulated genes in shades of blue. Of note, the majority of the mice included in the analysis were female.

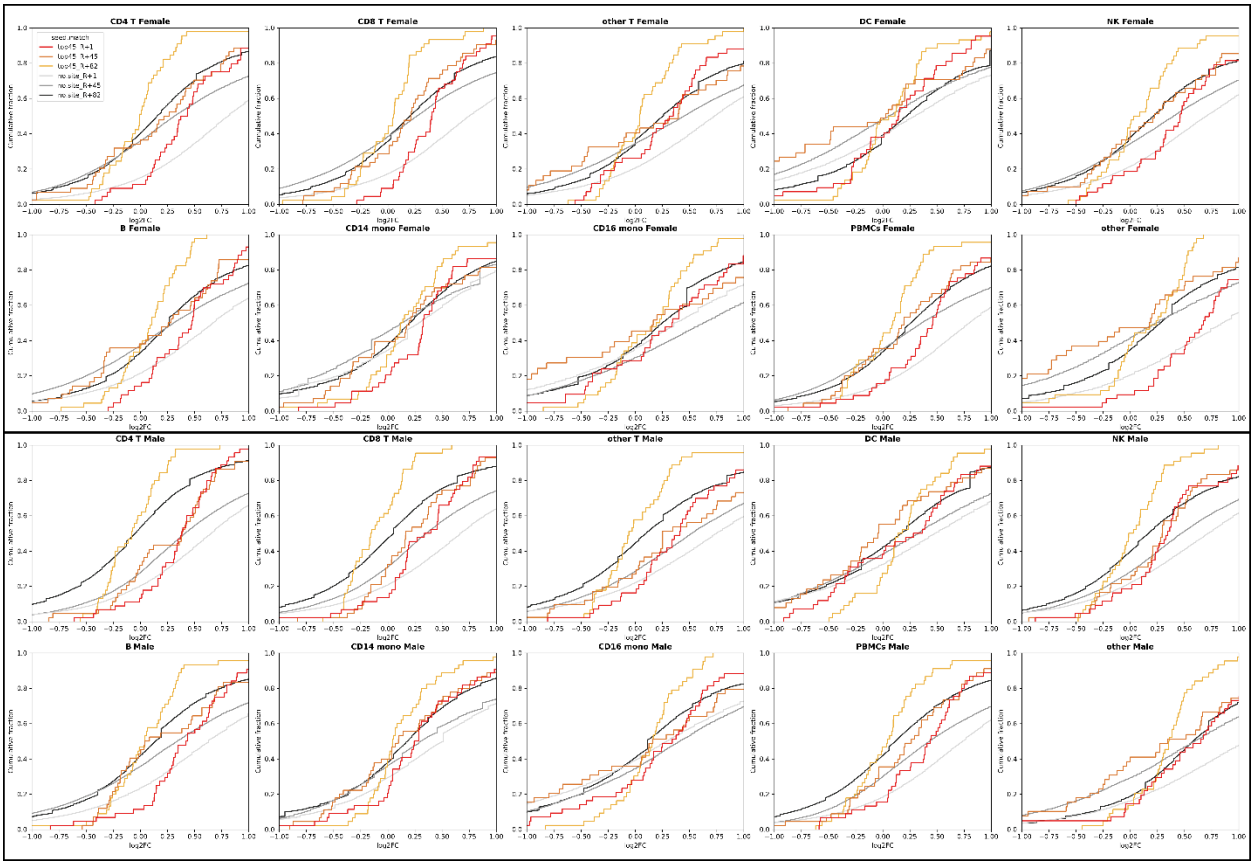

Supplementary Figure 11. Sex-specific cumulative plots illustrate the impact on the top 45 gene targets of 13 specific miRNAs in Inspiration 4 (I4) astronaut data, derived from scRNA-sequence analysis of whole blood. Cumulative plots for the different cell types from the the I4 astronaut scRNA-seq data, comparing 1 day after return to Earth (R1) (red line), 45 days after return to Earth (R45) (orange line), and 82 days after return to Earth (R82) (gold line) to pre-flight levels. The x-axis represents $\log_2$(fold-change) values for the comparisons, while the "no-site" line serves as a baseline for genes without targets to the 13 miRNAs. Various shades of grey in the no-site lines correspond to specific comparisons, as indicated in the figure legend. The top cumulative plots are specifically for the female astronauts, while the bottom cumulative plots are specifically for the male astronauts

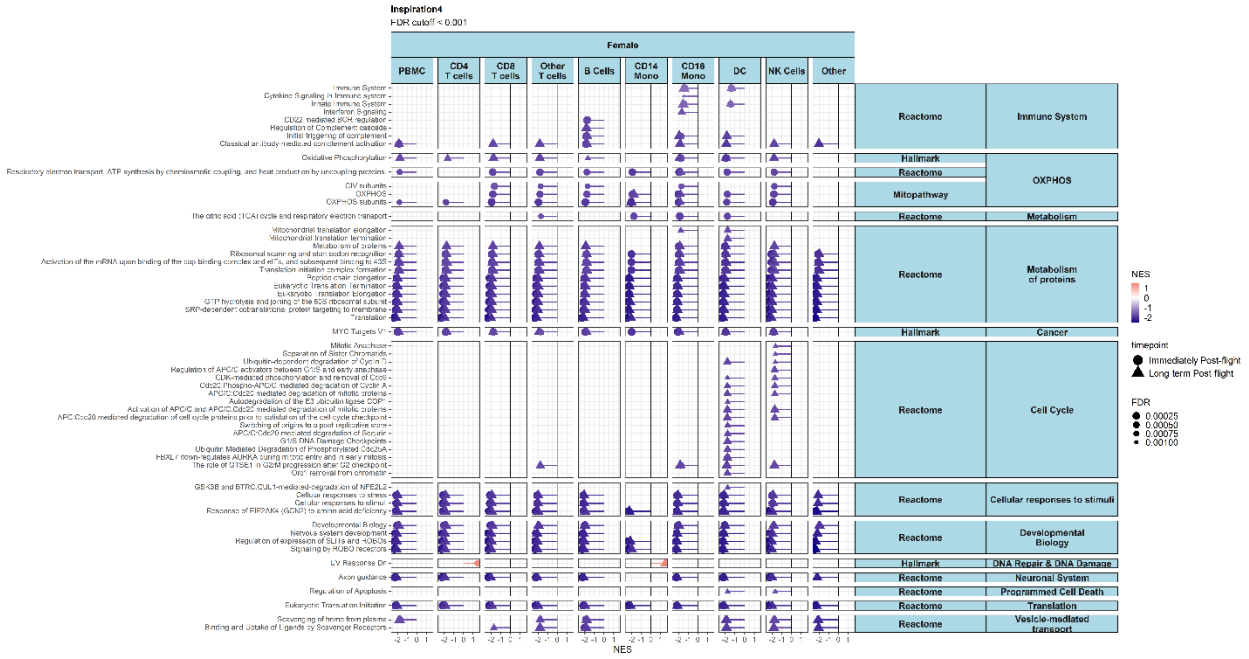

Supplementary Figure 12. Pathways similar to the 13 miRNA gene target pathways from Fig. 4 from analysis on the Inspiration4 (I4) female astronauts. This lollipop plot represents fast Gene Set Enrichment Analysis (fGSEA) of differential gene expression (DGE) data from scRNA-seq data on the blood samples of the female I4 astronauts comparing immediate post-flight (1 day after return to Earth) vs preflight (circles) and long-term post-flight (45 and 84 days after returning to Earth) vs preflight (triangles). fGSEA was performed using the Hallmark, Reactome, and MitoCarta pathway databases. The plot highlights pathways similar to those identified in the functional pathway analysis of the 13 miRNAs in **Figure 4**, showing that similar pathways are dysregulated in female astronauts after returning to Earth. The x-axis represents the Normalized Enrichment Score (NES), with negative values (shades of blue) indicating pathway inhibition and positive values (shades of red) indicating pathway activation. Point size reflects the degree of significance, denoted by the False Discovery Rate (FDR). Only significant values (FDR < 0.001) are displayed. The complete list of pathway analyses is available in **Supplementary Data 3**.

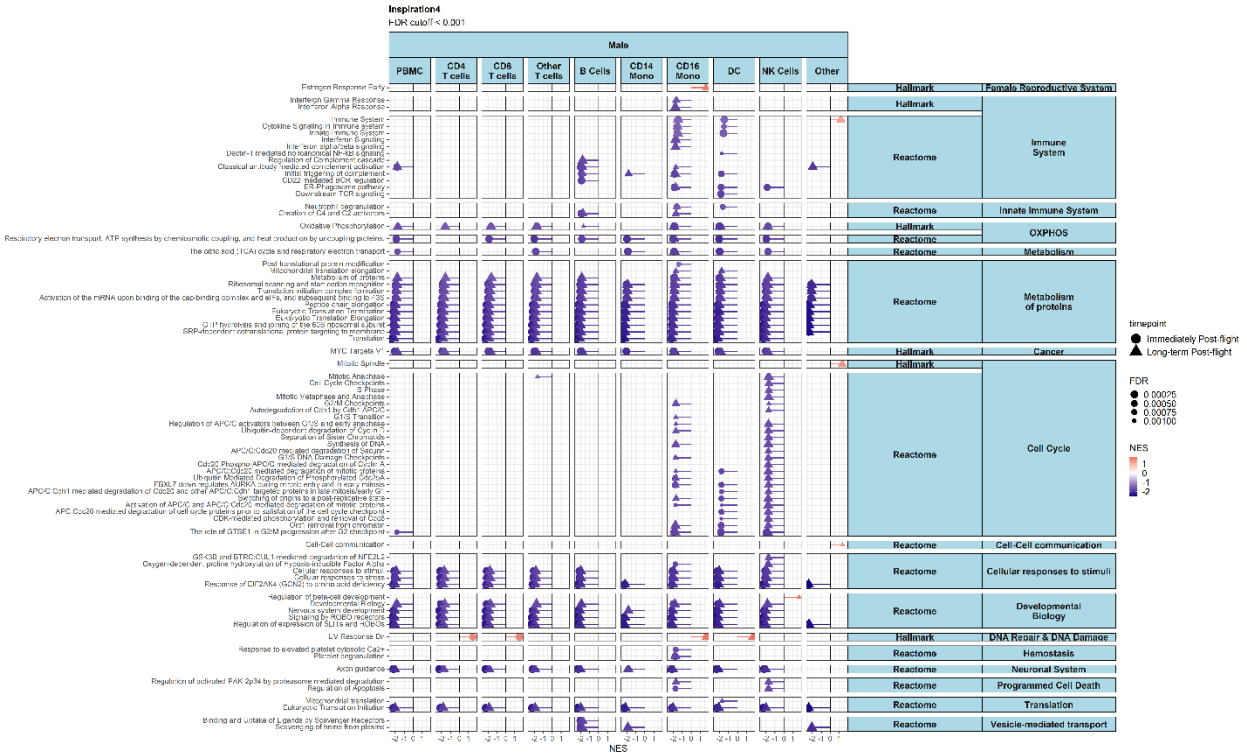

Supplementary Figure 13. Pathways similar to the 13 miRNA gene target pathways from Fig. 4 from analysis on the Inspiration4 (I4) male astronauts. This lollipop plot represents fast Gene Set Enrichment Analysis (fGSEA) of differential gene expression (DGE) data from scRNA-seq data on the blood samples of the male I4 astronauts comparing immediate post-flight (1 day after return to Earth) vs preflight (circles) and long-term post-flight (45 and 84 days after returning to Earth) vs preflight (triangles). fGSEA was performed using the Hallmark, Reactome, and MitoCarta pathway databases. The plot highlights pathways similar to those identified in the functional pathway analysis of the 13 miRNAs in **Figure 4**, showing that similar pathways are dysregulated in female astronauts after returning to Earth. The x-axis represents the Normalized Enrichment Score (NES), with negative values (shades of blue) indicating pathway inhibition and positive values (shades of red) indicating pathway activation. Point size reflects the degree of significance, denoted by the False Discovery Rate (FDR). Only significant values (FDR < 0.001) are displayed. The complete list of pathway analyses is available in **Supplementary Data 3**.

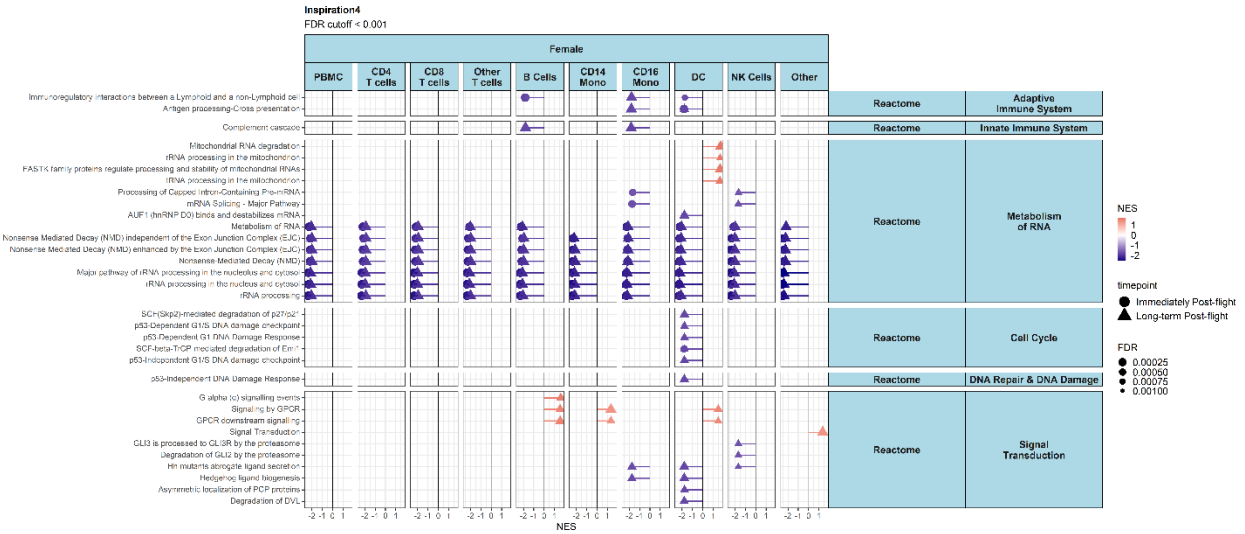

Supplementary Figure 14. Pathways similar to the 45 gene target pathways from Fig. 5 from analysis on the Inspiration4 (I4) female astronauts. This lollipop plot represents fast Gene Set Enrichment Analysis (fGSEA) of differential gene expression (DGE) data from scRNA-seq data on the blood samples of the female I4 astronauts comparing immediate post-flight (1 day after return to Earth) vs preflight (circles) and long-term post-flight (45 and 84 days after returning to Earth) vs preflight (triangles). fGSEA was performed using the Hallmark and Reactome pathway databases. The plot highlights pathways similar to those identified for the 45 gene targets for the 13 miRNAs in **Figure 5**, showing that similar pathways are dysregulated in female astronauts after returning to Earth. The x-axis represents the Normalized Enrichment Score (NES), with negative values (shades of blue) indicating pathway inhibition and positive values (shades of red) indicating pathway activation. Point size reflects the degree of significance, denoted by the False Discovery Rate (FDR). Only significant values (FDR < 0.001) are displayed. The complete list of pathway analyses is available in **Supplementary Data 3**.

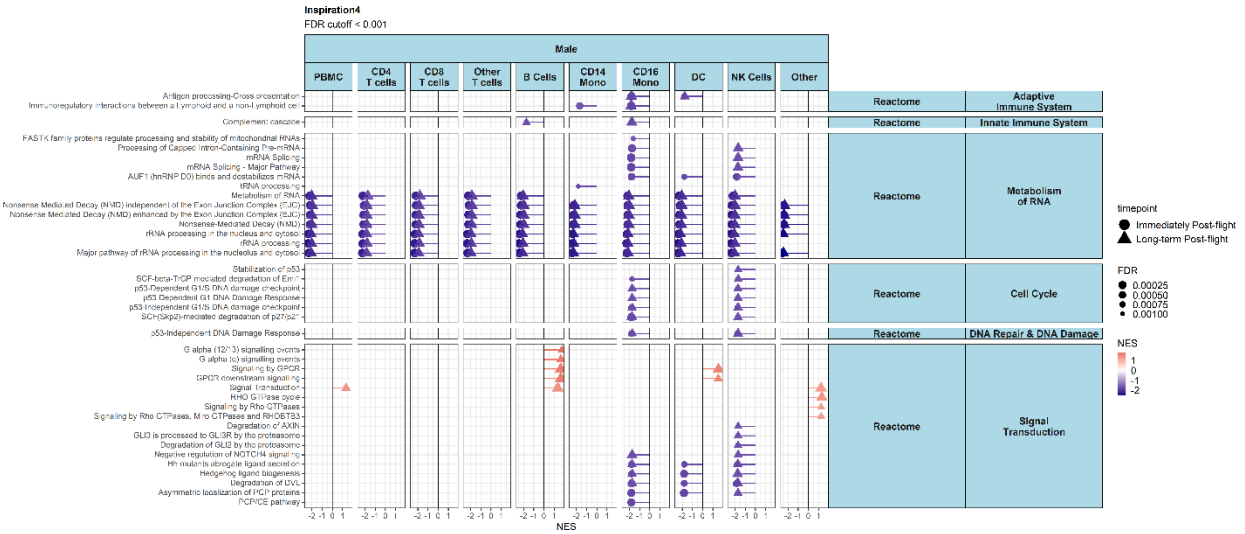

Supplementary Figure 15. Pathways similar to the 45 gene target pathways from Fig. 5 from analysis on the Inspiration4 (I4) male astronauts. This lollipop plot represents fast Gene Set Enrichment Analysis (fGSEA) of differential gene expression (DGE) data from scRNA-seq data on the blood samples of the male I4 astronauts comparing immediate post-flight (1 day after return to Earth) vs preflight (circles) and long-term post-flight (45 and 84 days after returning to Earth) vs preflight (triangles). fGSEA was performed using the Hallmark and Reactome pathway databases. The plot highlights pathways similar to those identified for the 45 gene targets for the 13 miRNAs in **Figure 5**, showing that similar pathways are dysregulated in female astronauts after returning to Earth. The x-axis represents the Normalized Enrichment Score (NES), with negative values (shades of blue) indicating pathway inhibition and positive values (shades of red) indicating pathway activation. Point size reflects the degree of significance, denoted by the False Discovery Rate (FDR). Only significant values (FDR < 0.001) are displayed. The complete list of pathway analyses is available in **Supplementary Data 3**.

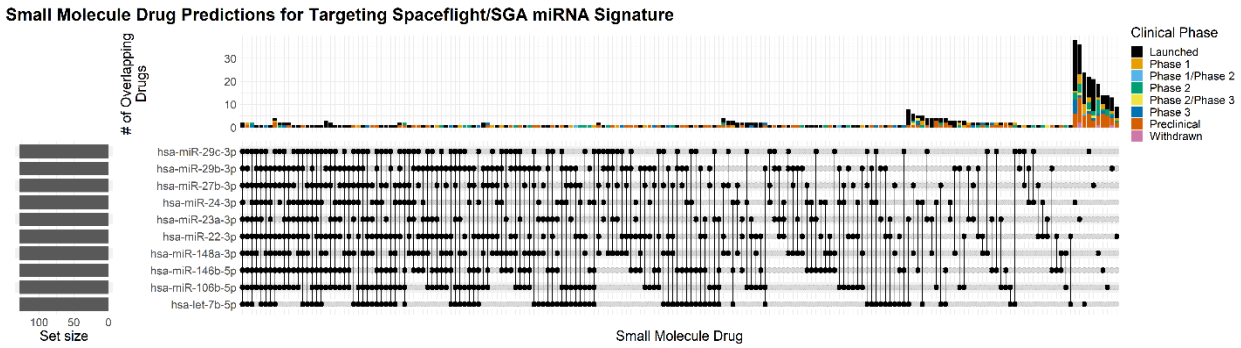

Supplementary Figure 16. Predicted small molecule drugs for SGA-associated spaceflight miRNA signature. Upset plot revealing specific predicted small molecule drugs that target the miRNA signature associated with Small-for-Gestational-Age (SGA) in spaceflight. The drug names and details can be found in **Supplementary Data 4**.

miRNA	Pollution	Diet	Exercise
hsa-miR-22-3p	↓ [1]	↑ (HFD) [2,3]	↓ [4]
hsa-miR-29c-3p	--	↑ (HFD) [5]	↓ [6]
let-7b-5p	↑ [7,8]	↑ (KD) [9]	↓ [6]
hsa-miR-27b-3p	↓ [10]	↑ (HFD) [11]	↑ [6]
hsa-miR-29b-3p	↑ [12]	--	↓ [6]
hsa-miR-106b-5p	↑ [13]	↓ (dairy) [14]	↓ [15]
hsa-miR-23a-3p	↑ [16]	↑ (sodium) [17]	↓ [18]
hsa-miR-130a-3p	↓ [19]	↑ (LFD) [20]	↓ [21]
hsa-miR-148a-3p	↓ [22]	--	↓ [18]
hsa-miR-24-3p	↓ [23]	↑ (HFD) [24]	↓ [18,25]
hsa-miR-378a-3p	--	↑ (HF, magnesium) [26,27]	↑ [27]
hsa-miR-192-5p	↑ [28]	↓ (HFD) [29]	↓ [30]
hsa-miR-146b-5p	↑ [31]	↓ (HFD) [11]	↓ [32]

Supplementary Table 1. Influence of environmental factors on the 13 miRNAs. Expression of the 13 miRNAs under the influence of pollution, diet and exercise: ↑ overexpressed, ↓ less expressed. We indicate for the diet: HFD (high-fat diet), LFD (low-fat diet), KD (ketogenic diet) and HF (high-fructose diet).

References

1. Zhong, S. & Borlak, J. Sex differences in the tumor promoting effects of tobacco smoke in a cRaf transgenic lung cancer disease model. *Arch Toxicol* **98**, 957–983 (2024).
2. Senese, R. *et al.* miR-22-3p is involved in gluconeogenic pathway modulated by 3,5-diiodo-L-thyronine (T2). *Sci Rep* **9**, 16645 (2019).
3. Gjorgjieva, M. *et al.* Genetic Ablation of MiR-22 Fosters Diet-Induced Obesity and NAFLD Development. *J Pers Med* **10**, 170 (2020).
4. Baraniuk, J. N. & Shivapurkar, N. Exercise – induced changes in cerebrospinal fluid miRNAs in Gulf War Illness, Chronic Fatigue Syndrome and sedentary control subjects. *Sci Rep* **7**, 15338 (2017).
5. Rojas-Criollo, M. *et al.* Effects of a High-Fat Diet on Insulin-Related miRNAs in Plasma and Brain Tissue in APPSwe/PS1dE9 and Wild-Type C57BL/6J Mice. *Nutrients* **16**, 955 (2024).
6. Barber, J. L. *et al.* The Effects of Regular Exercise on Circulating Cardiovascular-related MicroRNAs. *Sci Rep* **9**, 7527 (2019).
7. Deng, Q. *et al.* Co-exposure to metals and polycyclic aromatic hydrocarbons, microRNA expression, and early health damage in coke oven workers. *Environ. Int.* **122**, 369–380 (2019).
8. Chao, M.-W. *et al.* Exposure to PM2.5 causes genetic changes in fetal rat cerebral cortex and hippocampus. *Environ Toxicol* **32**, 1412–1425 (2017).
9. Cannataro, R. *et al.* Ketogenic Diet Acts on Body Remodeling and MicroRNAs Expression Profile. *Microrna* **8**, 116–126 (2019).
10. Zhang, J. *et al.* Complex molecular mechanism of ammonia-induced apoptosis in chicken peripheral blood lymphocytes: miR-27b-3p, heat shock proteins, immunosuppression, death receptor pathway, and mitochondrial pathway. *Ecotoxicology and Environmental Safety* **236**, 113471 (2022).
11. López-Pastor, A. R. *et al.* Concerted regulation of non-alcoholic fatty liver disease progression by microRNAs in apolipoprotein E-deficient mice. *Dis Model Mech* **14**, dmm049173 (2021).
12. Peng, Z. *et al.* MiR-29b-3p aggravates NG108-15 cell apoptosis triggered by fluorine combined with aluminum. *Ecotoxicol Environ Saf* **224**, 112658 (2021).

13. Xue, C. *et al.* MicroRNA-106b-5p participates in lead (Pb2+)-induced cell viability inhibition by targeting XIAP in HT-22 and PC12 cells. *Toxicol In Vitro* **66**, 104876 (2020).
14. Khorraminezhad, L. & Rudkowska, I. Dairy Product Intake Modifies MicroRNA Expression among Individuals with Hyperinsulinemia: A Post-Intervention Cross-Sectional Study. *Lifestyle Genom* **15**, 77–86 (2022).
15. Torres-Aguilera, I., Pinto-Hernandez, P., Iglesias-Gutierrez, E., Terrados, N. & Fernandez-Sanjurjo, M. Circulating plasma levels of miR-106b-5p predicts maximal performance in female and male elite kayakers. *Front Sports Act Living* **5**, 1040955 (2023).
16. Rodosthenous, R. S. *et al.* Ambient particulate matter and microRNAs in extracellular vesicles: a pilot study of older individuals. *Part Fibre Toxicol* **13**, 13 (2016).
17. Ferrero, G. *et al.* Intake of Natural Compounds and Circulating microRNA Expression Levels: Their Relationship Investigated in Healthy Subjects With Different Dietary Habits. *Front Pharmacol* **11**, 619200 (2020).
18. Sansoni, V. *et al.* Effects of repeated sprints training on fracture risk-associated miRNA. *Oncotarget* **9**, 18029–18040 (2018).
19. Mesnage, R., Mahmud, N., Mein, C. A. & Antoniou, M. N. Alterations in small RNA profiles in liver following a subchronic exposure to a low-dose pesticide mixture in Sprague-Dawley rats. *Toxicol Lett* **353**, 20–26 (2021).
20. Assmann, T. S., Riezu-Boj, J. I., Milagro, F. I. & Martínez, J. A. Circulating adiposity-related microRNAs as predictors of the response to a low-fat diet in subjects with obesity. *J Cell Mol Med* **24**, 2956–2967 (2020).
21. Garai, K. *et al.* Physical Activity as a Preventive Lifestyle Intervention Acts Through Specific Exosomal miRNA Species-Evidence From Human Short- and Long-Term Pilot Studies. *Front Physiol* **12**, 658218 (2021).
22. Shi, L. *et al.* Genome wide profiling of miRNAs relevant to the DNA damage response induced by hexavalent chromium exposure (DDR-related miRNAs in response to Cr (VI) exposure). *Environ Int* **157**, 106782 (2021).
23. Huang, S. *et al.* Polycyclic Aromatic Hydrocarbons-Associated MicroRNAs and Heart Rate Variability in Coke Oven Workers. *J Occup Environ Med* **58**, e24-31 (2016).
24. Ma, F. *et al.* Identification of novel circulating miRNAs biomarkers for healthy obese and lean children. *BMC Endocr Disord* **23**, 238 (2023).
25. Margolis, L. M. *et al.* Circulating and skeletal muscle microRNA profiles are more sensitive to sustained aerobic exercise than energy balance in males. *J Physiol* **600**, 3951–3963 (2022).
26. Sud, N. *et al.* Aberrant expression of microRNA induced by high-fructose diet: implications in the pathogenesis of hyperlipidemia and hepatic insulin resistance. *J Nutr Biochem* **43**, 125–131 (2017).
27. Krammer, U. D. B. *et al.* MiRNA-based “fitness score” to assess the individual response to diet, metabolism, and exercise. *J Int Soc Sports Nutr* **19**, 455–473.
28. Petri, B. J. *et al.* Multiomics analysis of the impact of polychlorinated biphenyls on environmental liver disease in a mouse model. *Environ Toxicol Pharmacol* **94**, 103928 (2022).
29. Liu, X.-L. *et al.* miR-192-5p regulates lipid synthesis in non-alcoholic fatty liver disease through SCD-1. *World J Gastroenterol* **23**, 8140–8151 (2017).
30. Qin, Z., Han, X., Ran, J., Guo, S. & Lv, L. Exercise-Mediated Alteration of miR-192-5p Is Associated with Cognitive Improvement in Alzheimer’s Disease. *Neuroimmunomodulation* **29**, 36–43 (2022).
31. Xu, T. *et al.* Dioxin induces expression of hsa-miR-146b-5p in human neuroblastoma cells. *J Environ Sci (China)* **63**, 260–267 (2018).
32. Dalle Carbonare, L. *et al.* Modulation of miR-146b Expression during Aging and the Impact of Physical Activity on Its Expression and Chondrogenic Progenitors. *Int J Mol Sci* **24**, 13163 (2023).

miRNAs	Expression of miRNA	Pathways/health risks present in pregnant vs non-pregnant	References
hsa-miR-22-3p	↑ early pregnancy decidua, ↓ healthy pregnancy vs nonpregnant	early pregnancy decidua and menstrual endometria	[1,2]
hsa-miR-29c-3p	↑ pregnant women with complications leading to miscarriage	↓ COL4A1 and adhesive capacity leading to infertility	[3,4]
hsa-let-7b-5p	↓ neonatal encephalopathy, ↑ in Obese with Gestational Diabetes Mellitus (GDM), ↑ pregnant women with preterm birth	↑ apoptotic Hippo pathway	[5–7]
hsa-miR-27b-3p	↑ pregnancy resulting in fetal growth restriction, ↑ early onset preeclampsia	Targets APLN, EGFR, and FGF and involved in hypoxia	[8,9]
hsa-miR-29b-3p	↑ pregnant women developing GDM, ↑ pregnant women with preterm birth	Glucose	[7,10]
hsa-miR-106b-5p	↑ pregnant women who developed severe preeclampsia, ↑ maternal asthma during pregnancy, ↑ pregnant women with preterm birth	Cancer, cell cycle, TGF- β pathway	[7,11,12]
hsa-miR-23a-3p	↑ pregnant women with preterm birth	Targets Tbr1/Wnt pathways	[7,13]
hsa-miR-130a-3p	↑ pregnant women with preterm premature rupture of membranes vs healthy pregnant women	Altered collagen and matrix metalloprotease	[7,14]
hsa-miR-148a-3p	↑ pregnant women with complications leading to miscarriage and early- and late-onset pre-eclampsia	↓ TNF/IL1-0 levels and ↓ Treg	[15]
hsa-miR-24-3p	↑ pregnant women with severe preeclamptic pregnancies	TGF- β pathway, metabolic processes, cell cycle, MAP kinase signaling pathway	[16]
hsa-miR-378a-3p	↓ healthy pregnancy vs nonpregnant	N/A	[2]
hsa-miR-192-5p	↑ pregnant women developing GDM	Type 2 diabetes, inhibits epithelial transformation, suppresses uterine receptivity	[17,18]
hsa-miR-146b-5p	↑ early pregnancy decidua, ↓ pregnant women with complications leading to miscarriage	early pregnancy decidua and menstrual endometria, regulates inflammatory responses	[1,15,19]

Supplementary Table 2. The impact of the 13 miRNAs in pregnant women. A general literature review of the expression of these 13 miRNAs in the circulation of pregnant women. The expression levels are indicated with ↑ for upregulated and ↓ for downregulated. The pathways that the miRNAs are involved with during pregnancy are also indicated.

References

1. Lv, Y. *et al.* miRNA and target gene expression in menstrual endometria and early pregnancy decidua. *Eur J Obstet Gynecol Reprod Biol.* **197**, 27–30 (2016).
2. Légaré, C. *et al.* Human plasma pregnancy-associated miRNAs and their temporal variation within the first trimester of pregnancy. *Reprod Biol Endocrinol* **20**, 14 (2022).
3. Omeljaniuk, W. J., Laudański, P. & Miltyk, W. The role of miRNA molecules in the miscarriage process. *Biol Reprod* **109**, 29–44 (2023).
4. Griffiths, M., Van Sinderen, M., Rainczuk, K. & Dimitriadis, E. miR-29c overexpression and COL4A1 downregulation in infertile human endometrium reduces endometrial epithelial cell adhesive capacity in vitro implying roles in receptivity. *Sci Rep* **9**, 8644 (2019).
5. Ponnusamy, V. *et al.* Neuronal let-7b-5p acts through the Hippo-YAP pathway in neonatal encephalopathy. *Commun Biol* **4**, 1143 (2021).
6. Serati, A. *et al.* Characterization of Maternal Circulating MicroRNAs in Obese Pregnancies and Gestational Diabetes Mellitus. *Antioxidants* **12**, 515 (2023).
7. Cook, J. *et al.* First Trimester Circulating MicroRNA Biomarkers Predictive of Subsequent Preterm Delivery and Cervical Shortening. *Sci Rep* **9**, 5861 (2019).
8. Tagliaferri, S. *et al.* miR-16-5p, miR-103-3p, and miR-27b-3p as Early Peripheral Biomarkers of Fetal Growth Restriction. *Front Pediatr* **9**, 611112 (2021).
9. Gusar, V. *et al.* Preeclampsia: The Interplay between Oxygen-Sensitive miRNAs and Erythropoietin. *J Clin Med* **9**, 574 (2020).
10. Dinesen, S., El-Faitarouni, A. & Dalgaard, L. T. Circulating microRNAs associated with gestational diabetes mellitus: useful biomarkers? *J Endocrinol.* **256**, (2023).
11. Luizon, M. R. *et al.* Circulating MicroRNAs in the Second Trimester From Pregnant Women Who Subsequently Developed Preeclampsia: Potential Candidates as Predictive Biomarkers and Pathway Analysis for Target Genes of miR-204-5p. *Front Physiol* **12**, 678184 (2021).
12. Bozack, A. K. *et al.* Breast milk-derived extracellular vesicle miRNAs are associated with maternal asthma and atopy. *Epigenomics* **14**, 727–739.
13. Qin, D., Wang, C., Li, D. & Guo, S. Exosomal miR-23a-3p derived from human umbilical cord mesenchymal stem cells promotes remyelination in central nervous system demyelinating diseases by targeting Tbr1/Wnt pathway. *J Biol Chem* **300**, 105487 (2024).
14. Spiliopoulos, M. *et al.* MicroRNA analysis in maternal blood of pregnancies with preterm premature rupture of membranes reveals a distinct expression profile. *PLoS One* **17**, e0277098 (2022).
15. Winger, E. E., Reed, J. L. & Ji, X. First-trimester maternal cell microRNA is a superior pregnancy marker to immunological testing for predicting adverse pregnancy outcome. *J Reprod Immunol* **110**, 22–35 (2015).
16. Wu, L. *et al.* Circulating microRNAs are elevated in plasma from severe preeclamptic pregnancies. *Reproduction* **143**, 389–397 (2012).
17. Thamotharan, S. *et al.* Circulating extracellular vesicles exhibit a differential miRNA profile in gestational diabetes mellitus pregnancies. *PLoS One* **17**, e0267564 (2022).

18. Liang, J. *et al.* miR-192-5p suppresses uterine receptivity formation through impeding epithelial transformation during embryo implantation. *Theriogenology* **157**, 360–371 (2020).
19. Schjenken, J. E. *et al.* miRNA Regulation of Immune Tolerance in Early Pregnancy. *Am. J. Reprod. Immunol.* **75**, 272–280 (2016).